A Molecular Modeling Study of Binary Blend Compatibility of Polyamide 6 and Poly(vinyl acetate) with Different Degrees of Hydrolysis: An Atomistic and Mesoscopic Approach

Theodora Spyriouni and Caroll Vergelati*

Rhodia Recherches, Centre de Recherches de Lyon, BP 62, 69192, Saint-Fons Cedex, France

Received September 25, 2000; Revised Manuscript Received March 1, 2001

ABSTRACT: The binary blend compatibility of polyamide 6 (PA6) with poly(vinyl alcohol) (PVOH), poly(vinyl acetate) (PVAC), and partially hydrolyzed PVAC was studied for a wide range of compositions, by atomistic and mesoscopic modeling. The Flory−Huggins interaction parameter χ, calculated for these mixtures by atomistic modeling, showed that favorable interactions develop for PVAC with a low hydrolysis degree for a specific composition and also for compositions rich in either component. The effect of the PVAC hydrolysis degree on the mixture compatibility was explained in terms of the reduced ability of the acetylated chains to form hydrogen bonds, which in turn, may result in weaker intramolecular interactions. Such an effect may also be due to the more extended conformations assumed by these chains because of the bulky side groups. Calculations at high temperature gave small negative χ parameters, in good agreement with results reported by others. The χ and other structure-dependent parameters, derived from the atomistic level, were supplied to coarse-grained (mesoscopic) simulations. The length and time scales spanned by these simulations were relevant to real application scales. The kinetics of phase separation were examined via the structure factor and the growth rate of the domain size. Larger domain sizes were observed for the less hydrolyzed mixtures due to smaller χ parameters which implied higher temperature simulations for these mixtures. The exponent of the domain growth for the symmetric 1/1 and asymmetric 2/1 mixtures was found in the range 0.2−0.28 irrespective of time step. At equilibrium, the degree of order of the phases formed was extracted. This was found to decrease as the hydrolysis degree of PVAC decreased for a specific composition, indicating improved compatibility, in line with internal experimental findings and with results reported in the literature. The incompatible mixtures showed macrophase separation with a wide density spectrum. Compatibility was obtained for all PVAC/PA6 mixtures and also for the mixture of PVAC with 75% degree of hydrolysis for the composition 1/3 v/v, rich in PA6.

1. Introduction

The blending of different polymers has been widely used for obtaining products with desirable properties which are not necessarily possessed by one single polymer. The process of simple blending is attractive for industrial applications due to the low cost associated with the process, compared to the chemical modification (e.g., grafting) of existing polymers or the synthesis of new ones. However, readily miscible polymer mixtures are seldom obtained. The entropy of mixing is very small for long polymers, and thus favorable energetic interactions (hydrogen bonding, dipole interactions) between the different components are needed in order to avoid phase separation. In the case of copolymers with chemically distinct monomer units, the chemical bonds restrict the macroscopic separation. This leads to the formation of microscopic patterns of typical size 10−100 nm. The knowledge of the morphology formed by microscopically separated copolymer melts is important for the determination of the suitability of the final product for a specific application. Mean field theories and molecular simulation have proven to be valuable tools for studying the phase behavior of polymer systems and provide a reliable and fast means to screening candidate mixtures for a given application.

The self-consistent mean field theory[1−5] (SCFT) has led to significant advances in the microphase separation study of (mainly) diblock (the whole phase diagram has been calculated in good agreement with experimental results) and triblock copolymers. The whole range from weak to strong segregation limit has been investigated. The molecular parameters involved are the "incompatibility parameter" χN, where χ is the Flory−Huggins interaction parameter and N is the polymerization degree, and the composition parameter f defined as $f_A = N_A/N$, where N_A is the number of A monomers. More architectural parameters are required in order to account for block sequence and specific chain architecture. In the context of SCFT the polymers are modeled as Gaussian chains consisting of beads with equal statistical lengths, which interact via external fields that are related to the monomer densities via self-consistent equations. The problem consists of solving these equations for a presumed symmetry of the microstructure. The ordered structure that gives the lowest free energy is chosen to be the final morphology. Stable morphologies such as lamellae, hexagonal arrays of cylinders, body-centered cubic spheres, close packed spheres, bicontinuous phases, and their combinations in the case of triblock copolymers have been found to be in good agreement with experimental results.[6,7]

In contrast with the above type of "equilibrium" theories, dynamic approaches permit the modeling of morphology evolution in polymer systems during phase separation. Mesoscopic dynamics[8,9] (MesoDyn) and dissipative particle dynamics[10−12] (DPD) methods have been developed over the past decade. Both approaches treat the polymer chains in a coarse-grained (mesoscopic) level by grouping atoms together up to the persistence length of the polymers. This treatment can

10.1021/ma001669t CCC: $20.00
Published on Web 06/19/2001

extend the length and time scales by many orders of magnitude compared to the atomistic simulations. MesoDyn is a dynamic mean field density functional theory. The phase separation dynamics are described by Langevin-type equations for polymer diffusion and thermal fluctuations are added as noise (random force). The method has been applied with success to concentrated aqueous solutions of poly(ethylene oxide) − poly(polypropylene oxide) triblock copolymers[13] (trademark Pluronics). DPD is essentially a molecular dynamics (MD) method with added noise, similar to Brownian dynamics. In the DPD method the particles are subject to conservative, dissipative, and random forces which are calculated for pairs of neighboring particles. In contrast to classical MD, the method employs soft interaction potentials, as a natural consequence of the coarse-grained representation, allowing large time scale simulations. The time evolution of the system is found by solving Newton's equations of motion. The method leads to a correct description of the Navier−Stokes hydrodynamic behavior.[10]

In the present study, molecular simulations at both the atomistic and mesoscopic level were conducted for binary blends of polyamide 6 (PA6) and poly(vinyl acetate) (PVAC) of different hydrolyzation degrees. PA6 has been a frequently used polymer for blending applications due to the good mechanical properties it possesses. Several studies have appeared in the literature concerning the compatibility of polyamides with polymers containing vinyl alcohol (VOH) monomer units, which are capable of hydrogen-bond interactions. However, blending these polymers poses difficulties because of the tight intramolecular structure that they develop due to hydrogen bonding. In ref 14 random copolyamides were blended with PVOH and in refs 15 and 16 with poly(ethylene-*co*-vinyl alcohol). The random copolyamides are expected to have an improved compatibility by introducing a randomness in the intramolecular packing of the polyamide chains. Binary blends of PA6 with poly(ethylene-*co*-vinyl alcohol) were studied in ref 17 and with partially hydrolyzed PVAC in refs 18 and 19. More specifically, Ha et al.[18] examined the binary blend compatibility of PA6 with PVOH, partially hydrolyzed PVAC (34% VOH groups) and PVAC, in terms of melting temperature (T_m) depression and scanning electron micrography (SEM). SEM micrographs showed poor compatibility at the molecular level for all mixtures and for compositions 50/50 w/w. A later work of Koulouri and Kallitsis[19] studied the binary system of PA6 with PVOH and partially hydrolyzed PVAC (88% VOH groups). Thermal properties (such as T_m and glass transition temperature (T_g)) and mechanical properties (such as loss modulus, ultimate stress, and strain) were reported for a wide range of compositions. Evidence of compatibility was reported for the partially hydrolyzed PVAC mixtures for specific compositions.

The present study focused on binary blends of PA6 with PVOH, PVAC, and partially hydrolyzed PVAC (88% and 75% VOH groups). The compatibility of these blends was estimated by an approach that treated, hierarchically, the different length and time scales involved in the problem. First, molecular dynamics (MD) simulations of oligomers of the above systems were conducted at room temperature, and for a wide range of compositions. The cohesive energy density of the pure components and mixtures was calculated, and from there the χ interaction parameter was derived as a function of composition for the different blends. The χ values indicated favorable interactions for specific mixtures. This was further related to the functional groups of the chains by examining the ability of the various polyvinyl chains to form hydrogen bonds and by inspecting short scale conformational characteristics (dihedral angles). The interaction parameters obtained from the atomistic simulations along with other structure-dependent (monomer number and length; characteristic ratio) parameters were, subsequently, supplied into mesoscopic simulations. The short scale characteristics were, now, absorbed into large structureless beads. The coarse-grained representation of the systems at this level permitted the study of blends of high molecular weight (MW) and for time scales that allowed the observation of phase separation. The degree of order (order parameter) of the phases formed was derived. The results were compared qualitatively with results reported in the literature and with internal experimental findings.

In the following section are given the simulation details. The system of interest is presented in section 2.1, the atomistic simulation details in section 2.2, and the methodology and parametrization of the mesoscopic simulations in section 2.3. The results of the atomistic and mesoscopic simulations are discussed in section 3. The conclusions are summarized in section 4.

2. Simulation Details

2.1. System. The systems under consideration were binary blends of PA6 with PVOH, PVAC, and partially hydrolyzed PVAC (h-PVAC). Two types of h-PVAC were examined which contained 88% (h88-PVAC) and 75% (h75-PVAC) VOH groups, respectively. Both are commercially available. The binary blends of PVOH, h88-PVAC, and h75-PVAC were studied at PA6 volume fractions of 0.25(3/1), 0.32(2/1), 0.48(1/1), 0.66(1/2), and 0.75(1/3). The ratios in parentheses indicate the approximate volume proportions of PVOH (or h-PVAC)/PA6. The PVAC mixtures were at PA6 volume fractions of 0.35(2/1), 0.52(1/1), and 0.66(1/2). Note that the ratios in parentheses are used for convenience and they may correspond to volume fractions that are different from those mentioned above. All simulations were conducted at room temperature ($T = 298$ K).

2.2. Atomistic Simulations. Initially, the bulk phases were constructed with the Amorphous_Cell program of InsightII version 4.0, developed by Molecular Simulations Inc. (MSI). This program makes combined use of an algorithm developed by Theodorou and Suter[20] and the *scanning method* of Meirovitch.[21] In the seminal work of Theodorou and Suter, an amorphous phase of a glassy polymer is created in two stages. The conformations of the chains are assumed to resemble those of the unperturbed (from excluded volume interactions) chains that are found with significant probability in the bulk. Thus, initially, a proposed structure can be generated by using the rotational isomeric state (RIS) theory that describes the conformations of the unperturbed chains. To avoid excessive overlaps between the chains, modified conditional probabilities are used that account for the nonbonded interactions between the atom to be placed and the rest of the system. Subsequently, the initial structures are minimized by turning on, progressively, the potential energy interactions in a manner such that the more severe overlaps are relaxed first

(atom radii of half the actual size and no-rotational barriers) and, gradually, the minimum is reached by switching on the full potential (radii of actual size, rotational barriers, and attractive interactions). In the *scanning method*, all possible continuations of the growing chain are taken into account in the calculation of the conditional probabilities. In practice, the lookahead is restricted to a few backbone bonds (here three bonds were assumed).

After the initial construction, the amorphous phases were checked for filling space regularly and for a good "blending" of the different component chains. If in an initial configuration the two component chains were not well "mixed" (sufficient intermolecular contacts), then the configuration was discarded and a new one was attempted. In the case of irregular chain distribution ("holes", etc.), the initial configurations were refined by short dynamics simulations (up to 20 ps), followed by minimizations. The minimization procedure started with the steepest descent algorithm (away from the minimum) followed by the conjugate gradient algorithm (as the minimum was approached), until the energy had reached a minimum according to a predefined criterion (the root-mean-square of the components of the potential energy gradient was 0.1 kcal/mol/Å or less).

The interatomic interactions were modeled with the COMPASS[22] (condensed-phase optimized molecular potentials for atomistic simulation studies) force field (version 1.0) of MSI. This is an all-atom force field optimized to predict structural, conformational, and thermophysical condensed phase properties for the most common organic (and inorganic) molecules, including polymers. COMPASS is based on the PCFF (polymer consistent force field) force field. The energy expression comprises a combination of valence terms, including diagonal and cross-coupling terms for bond stretching, bond angle bending, and dihedral angle distortions, a Coulombic term for the electrostatic interactions and a Lennard-Jones 9−6 function for the van der Waals interactions.

For the calculation of the nonbonded interactions the cell multipole method[23−25] was used. This recently developed method has proven very efficient for the simulation of big systems since it scales linearly with the number of atoms N (compared to the cutoffs that scale as N^2) and requires modest memory. According to the method the periodic box is divided into M cubic cells with $M \approx N/4$ (optimum choice[25]). For each cell, the cells in the nearest neighborhood (26 cells for cubic systems) contribute to the near-field potential and the others to the far-field potential (short- and long-range interactions). The potential describing each cell has a general form that applies to both Coulombic and London dispersion interactions. The interactions between the atoms in the near-field cells are calculated directly for each pair of atoms. For the atoms in the far-field cells, the interactions are computed via expansions of multipole moments (charge, dipoles, quadrupoles, octopoles) around the center of each cell. The Taylor coefficients of the expansions are calculated only for each cell (and not for each atom) since it is assumed that the interactions of the atoms in the central cell with the far-field atoms vary little from one atom position to another (compared to the interactions between the near-field atoms). To reduce further the time spent on the calculation of the interactions due to the distant cells, a hierarchy of cells is implemented which increases the size of cells as the distance from the central cell increases (the cell size to the distance ratio remains constant). Also, in the multipole expansion, the octopole and/or quadrupole terms can be neglected. In the present work, a second-order multipole expansion was used (charges and dipoles), which gives reasonable accuracy with low overhead.

The amorphous phases contained oligomers of 16 monomer units for the PVOH, PVAC, and h-PVAC (32 backbone carbon atoms) and 6 monomer units for the PA6 (36 backbone carbon atoms). The h-PVAC chains were modeled as random sequences of VOH and VAC repeat units, according to the desired percentage of VOH groups (degree of hydrolysis). The density of each mixture was estimated on the basis of the pure component densities and by assuming volume additivity. The densities of the pure PVOH, h88-PVAC, and h75-PVAC were assumed to be the same and, along with the density of PA6, were taken from ref 19 as $\rho(\text{PVOH}) = 1.274$ g/cm^3 and $\rho(\text{PA6}) = 1.123$ g/cm^3. The notation of ref 19 is kept here, although with PVOH these authors mean the h88-PVAC. Their calculation was based on the degree of crystallinity observed and the densities of the amorphous ($\rho(\text{aPA6}) = 1.084$ g/cm^3, $\rho(\text{aPVOH}) = 1.26$ g/cm^3) and crystalline polymers ($\rho(\text{cPA6}) = 1.23$ g/cm^3, $\rho(\text{cPVOH}) = 1.35$ g/cm^3). In the present work, the same density was used for the three oligomers having neighboring degrees of hydrolysis (100%, 88% and 75%). The density of the pure PVAC was taken from ref 26 as $\rho(\text{PVAC}) = 1.191$ g/cm^3. The system size was typically 1000−2000 atoms, which is usually sufficient for avoiding finite size effects.[22] The box length was between 21 and 25 Å.

All simulations were carried out at room temperature. At this temperature, the oligomer chains were expected to be in a "frozen-in" state, since the high MW compounds are below their glass transition temperature. The T_g's of PA6, PVOH, and PVAC are 323−348, 343−372, and 301 K, respectively.[26] Thus, each system would be confined to fluctuate in the vicinity of the energy minimum where it is brought initially. To calculate the properties of interest (mainly cohesive energy densities), different initial configurations which sampled different areas of the phase space (this was checked visually and by the system energy) were generated for each system and relaxed, as described above. For each configuration, MD simulations under constant temperature and density (NVT ensemble), were conducted by using the Discover3 program of InsightII, developed by MSI. The temperature was controlled by direct velocity scaling. The Verlet leapfrog algorithm was used for the integration of the equations of motion and the time step was taken to be equal to 1 fs. Preliminary runs of 200−250 ps were carried out in order to bring the system to the target temperature. At the end of these runs, the energy of the system was monitored in order to ensure that it fluctuated around an average value. This was considered as a criterion for having "equilibrated" the system to the desired temperature. Main runs of 100 ps followed, during which trajectories were stored, periodically, for later postprocessing. For each type of mixture and composition studied, five to seven trajectories were generated, starting from different initial configurations. The mean values were estimated as arithmetic averages over the configurations stored in each trajectory and over all trajectories generated for each system. With this method, thermal fluctuations were taken into account

in contrast to the standard molecular mechanics where averages are calculated over static minimum energy configurations.[20] This leads to more reliable estimates of properties at the temperature of interest. It is noted, however, that at the low temperature of examination, the systems were not in thermodynamic equilibrium and estimation of other properties such as pressure or properties dependent on the relaxation of long range conformational characteristics of the chains (radius of gyration, end-to-end distance) would be unreliable.

2.3. Mesoscopic Simulations. 2.3.1. Method. The phase separation dynamics at the mesoscopic level was simulated by using the MesoDyn program incorporated in the Cerius[2] programs of MSI. The approach[8,9] is a dynamic variant of the mean-field density functional theory. The theory underlying the methodology is similar to the classical dynamic random phase approximation (RPA).[27,28] The polymer chains are modeled as ideal Gaussian chains consisting of beads. Each bead represents a number of monomers of the real polymer, equal to the characteristic ratio of the polymer (Kuhn statistical segments). The nonideal interactions between the chains are introduced by a mean field potential F^{nid} which has the form

$$F^{\mathrm{nid}}[\rho] = \frac{1}{2}\sum_{IJ}\int_V\int_V \epsilon_{IJ}(\mathbf{r}-\mathbf{r}')\rho_I(\mathbf{r})\rho_J(\mathbf{r}')\,\mathrm{d}\mathbf{r}\,\mathrm{d}\mathbf{r}' \quad (1)$$

where $\rho_I(\mathbf{r})$ is the density of bead type I at $\mathbf{r}$ (local bead concentration), and $\epsilon_{IJ}(\mathbf{r}-\mathbf{r}')$ is a cohesive interaction between beads I at $\mathbf{r}$ and J at $\mathbf{r}'$, chosen to have a Gaussian form

$$\epsilon_{IJ}(\mathbf{r}-\mathbf{r}') = \epsilon_{IJ}^0\left(\frac{3}{2\pi\alpha^2}\right)^{3/2} \mathrm{e}^{-(3/2\alpha^2)(\mathbf{r}-\mathbf{r}')^2} \quad (2)$$

where α is the Gaussian bond length and ϵ_{IJ}^0 is the constant cohesive interaction between beads I and J which can be taken to be equal to the Flory−Huggins χ parameter.

If additional external potentials $U_I(r)$ are coupled to the Hamiltonian of the system in order to constrain the density fields $\rho_I(\mathbf{r})$ to the observed densities $\rho_I^0(\mathbf{r})$, then a free energy functional can be defined as

$$F[\psi] = \mathrm{Tr}(\psi H^{\mathrm{id}} + \beta^{-1}\psi \ln \psi) + \sum_I\int_V U_I(\mathbf{r})\,[\rho_I[\psi](\mathbf{r}) - \rho_I^0(\mathbf{r})]\,\mathrm{d}\mathbf{r} + F^{\mathrm{nid}}[\rho^0] + \lambda[\mathrm{Tr}\ \psi - 1] \quad (3)$$

ψ is the distribution of the bead positions (configurational distribution), H^{id} is the Hamiltonian of a Gaussian chain, and the term $\beta^{-1}\,\psi \ln \psi$ is the entropy of the distribution. Tr is defined as $1/(n!\Lambda^{3nN}) \int \mathrm{d}r_{11} \ldots \mathrm{d}r_{nN}$, where Λ is the de Broglie thermal wavelength, n the number of chains, and N the number of beads per chain. The last term in the above equation normalizes the distribution ψ (λ is a Lagrange multiplier).

The minimization of the free energy with respect to ψ leads to a configurational distribution that is determined by the external potentials $U_I(r)$. At every time step, the distribution ψ is the one that minimizes the free energy and constrains the density fields. In turn, the density fields $\rho_I(r)$ are determined by ψ. This results in the (important for the method) "bijectivity" concept, that is a one to one relation between the external potentials and the density fields.

When the system is away from equilibrium, the density fields evolve according to Langevin-type stochastic diffusion equations

$$\frac{\mathrm{d}\rho_I(\mathbf{r})}{\mathrm{d}t} = M\nabla\rho_I(\mathbf{r},t)\nabla\mu_I(\mathbf{r},t) + n \quad (4)$$

The first term on the right-hand side is the diffusion term. The gradient of the intrinsic chemical potentials μ_I is the thermodynamic force that drives the system to equilibrium. μ is derived from the differentiation of the free energy (eq 3) with respect to the density. This, in fact, results in a correlation between the chemical potential, the external potential, and the nonideal mean-field potential.[9]

$M\rho_I$, in the above equation, are the kinetic coefficients which are local and uncoupled. M is equal to βD, where D is the bead diffusion coefficient. A more realistic choice of the kinetic coefficients accounting for hydrodynamic interactions has been attempted by the same group.[29] In that work a modified Langevin equation was introduced and Darcy's law was used, which set the particle velocities proportional to an average external force.[30]

The second term on the right-hand side of eq 4 is the random force (noise) added to the system. The physical origin of this term is to deal with the fast degrees of freedom (Brownian particle with a heat bath). The noise satisfies the fluctuation−dissipation theorem.[28] By assuming incompressibility for a two-component system, i.e., $\nu^{-1} = \rho_I(\mathbf{r},t) + \rho_J(\mathbf{r},t)$, where ν is the molecular volume, eq 4 is transformed into the following exchange Langevin equations:[9]

$$\frac{\mathrm{d}\rho_I}{\mathrm{d}t} = M\nu\nabla\rho_I\rho_J\nabla[\mu_I - \mu_J] + n \quad (5)$$

$$\frac{\mathrm{d}\rho_J}{\mathrm{d}t} = M\nu\nabla\rho_I\rho_J\nabla[\mu_J - \mu_I] - n \quad (6)$$

The integration of the above equations is performed on a cubic lattice using a Crank−Nicolson numerical scheme.[31]

2.3.2. Parametrization. The polymer chains were mapped onto Gaussian chains by demanding the mean square end-to-end distance and the length of a fully extended (all trans) chain be equal for the real and the Gaussian chain. Thus, the number (N_b) and the length (α_b) of the Gaussian chain segments were estimated by the relationships

$$N_b = \frac{N_{\mathrm{mon}}}{C_\infty} \quad (7)$$

$$\alpha_b = \alpha_{\mathrm{mon}}C_\infty \quad (8)$$

where N_{mon} is the polymerization degree, α_{mon} is the monomer unit length, and C_∞ is the characteristic ratio of an infinite length chain.

The polymerization degree was determined by considering the following molecular weights: M_n(PVOH) = M_n(h88-PVAC) = M_n(h75-PVAC) = 67000 g mol^{-1},[19] M_n(PVAC) = 64800 g mol^{-1},[18] and M_n(PA6) = 20600 g mol^{-1}.[19] The C_∞ values were estimated from the SYNTHIA program of Cerius[2]. This semiempirical method,[32] developed by Bicerano, uses connectivity indices to describe the topology of the polymer. Four connectivity

Table 1. Binary Mixture Interaction Parameter χ Estimated from MD Simulations for Specific Compositions[a]

	χ					ϵ^0				
binary blend	3/1	2/1	1/1	1/2	1/3	3/1	2/1	1/1	1/2	1/3
PVOH/PA6	0.36_{11}	0.39_{11}	0.42_{9}	0.29_{11}	0.25_{6}	5.76	6.16	6.66	4.64	3.95
h88-PVAC/PA6	0.12_{11}	0.19_{12}	0.23_{12}	0.17_{10}	0.10_{8}	1.85	2.93	3.54	2.57	1.63
h75-PVAC/PA6	0.08_{7}	0.14_{11}	0.14_{8}	0.10_{11}	0.03_{8}	1.24	2.00	2.05	1.52	0.41
PVAC/PA6		0.01_{6}	0.02_{7}	0.01_{6}			0.12	0.19	0.12	

[a] All values refer to $T = 298$ K. Scaled interaction parameter ϵ^0 in kJ/mol.

indices are calculated, i.e., two atomic indices which are defined by the bonding and electronic environment of each non-hydrogen atom in a chain, and two bonding indices given in terms of the atomic indices. The properties are then derived from correlations of the connectivity indices. The C_∞ values for the hydrolyzed PVAC chains were estimated by considering random copolymers of VOH and VAC monomer units, at specific ratios. The C_∞ estimates for the PVOH, h88-PVAC, h75-PVAC, PVAC, and PA6 were found to be 6.86, 7.0, 7.19, 8.65, and 6.06, respectively. The monomer unit lengths of the polyvinyl chains were all taken to be 2.67 Å and the PA6 monomer unit length was taken as 8.99 Å.

In the present parametrization, the partially hydrolyzed PVAC chains which, in reality, constitute statistical copolymers of VOH and VAC units, were modeled as pseudo-homopolymer chains with all sites on a chain having the same size and interactions with sites on other chains. The influence of the same size approximation is marginal because of the similar size (monomer unit length) and characteristic ratio of the VOH and VAC repeat units. In terms of interactions, a mean energetic parameter was assigned at each site of a pseudo-homopolymer chain. This was the χ parameter taken from the detailed atomistic simulations conducted for each binary blend at each composition (section 2.2). Alternatively one could model the hydrolyzed chains as statistical copolymers and assign at each VOH or VAC site the interaction energy calculated for the PVOH/PA6 and PVAC/PA6 blends, respectively (see also Table 1). However, preliminary calculations of the number of Gaussian beads needed to represent each type of monomer for the h88-PVAC chains yielded a ratio of 1.5 VAC per 25 VOH beads. Thus, in such a model the compatibilizing effect of the VAC units would be unnoticeable.

The N_b and α_b of the Gaussian chains were calculated from eqs 7 and 8. These initial estimates were scaled in order to result into shorter chains with corresponding longer Gaussian bond lengths, i.e., N beads of length X where scaled to N/n beads with length nX, where n can be any integer that brings the number of beads down to a reasonable value (the computational time scales linearly with the number of beads). In the currently used program, only one α_b could be defined for each binary blend, and this was taken to be the arithmetic mean value of the bond lengths calculated for each polymer. This was a drastic approximation for the blends under consideration because of the different size of the polyvinyl and polyamide repeat units. To compensate for this innacuracy the number of beads for each polymer was further scaled (multiplied or divided) by the same factor the corresponding bond length was brought to the average value. The resulting estimates for the N_b of PVOH, h88-PVAC, h75-PVAC, and PA6 (in their binary mixtures) were 28, 25, 23, and 11, respectively. The average α_b for the above mixtures was taken equal to 14.6 nm. For the PVAC/PA6 binary blend the N_b estimates were 17 and 14, respectively, while the α_b was set to 11.6 nm. In all cases, the bond lengths were well above the persistence length of the polymers.

Table 2. Solubility Parameter (δ_{calc}) of High Molecular Weight PVOH, PVAC, and PA6 Estimated from Extrapolation of Data Obtained from Atomistic *NVT* Simulations of Oligomers, at Temperature $T = 298$ K and Density ρ[a]

	ρ (g/cm^3)	δ_{calc}	δ_{exp}[26]
PVOH	1.274	27.0	25.8−29.1
PVAC	1.191	17.7	19.1−22.6
PA6	1.123	24.7	22.5

[a] Experimental values (δ_{exp}) are shown for comparison. δ is expressed in $(J/cm^3)^{1/2}$.

The χ interaction parameters (Table 1) were calculated from atomistic simulations as described previously. These values characterized the nonideal interactions between the statistical segments (beads). Since the number of beads was scaled, the χ had to be scaled accordingly in order to result in a constant χN_b. For block copolymers it has been shown that the product χN_b drives the phase separation.[1−5] The scaled χ (ϵ^0) in units of KJ/mol are also given in Table 1.

The time step of the simulations was chosen so that a dimensionless time step τ used by the program was between 0 and 1 for numerical stability. This was defined as $\tau = \beta^{-1}Mh^2t$, where h is the cell size having an optimal value of 0.1543α, where α is the bond length.[9] Thus, the time step for the PVAC/PA6 mixture was chosen as 1.4 μs and for the rest of the systems as 2.4 μs. Another input parameter was the so-called size expansion parameter $\Omega = \nu^{-1}h^3$, where ν is the molecular volume (see 2.3.1). This parameter gives the number of beads at each cell and, thus, determines the influence of the noise. If it is chosen too low the noise level is high and the system is unstable, if it is too high the system freezes. Here, it was set equal to 100, a value that has been applied to short chains with long statistical units.[9] The distribution of the noise was taken to be uniform. For the integration of the dynamic equations (eqs 5 and 6) the periodic box was divided into $32 \times 32 \times 32$ cells. The periodic box for the PVAC/PA6 mixture measured around 323 nm at each side, and for the other mixtures 406 nm.

3. Results and Discussion

3.1. Atomistic Simulations. As a first step, the ability of the force field to predict the cohesive properties of the systems under consideration, was examined. Atomistic *NVT* simulations were performed for homologous series of pure PVOH, PVAC, and PA6. The densities of the pure component phases are given in Table 2. They were assumed independent of chain length and equal to the densities of the high MW homologues. From the *NVT* simulations the cohesive energy density (ced)

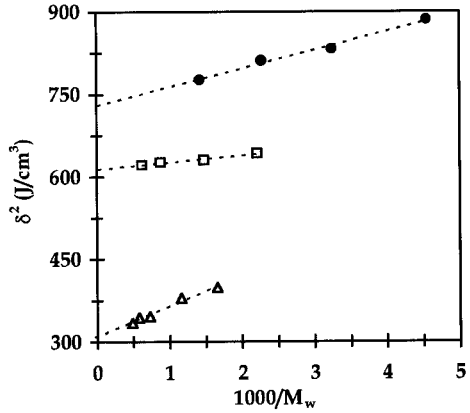

Figure 1. Square of the solubility parameter as a function of the reciprocal molecular weight of pure PVOH (circles), PA6 (squares), amd PVAC (triangles). The dotted lines indicate the extrapolation to infinite molecular weight.

was calculated as the mean total potential energy of intermolecular interactions. For each oligomer, the mean ced resulted as the arithmetic average of the ced values obtained from *NVT* simulations of different initial configurations, as described in section 2.2. In Figure 1 is plotted the square of the solubility parameter δ(ced) vs the reciprocal MW of the oligomers. As has been shown for other systems,[22] the extrapolation to infinite MW yields estimates that can be compared well with experimental solubility parameters of high polymers, given an appropriate force field. The values estimated from extrapolation are shown in Table 2, along with experimental data[26] for comparison. The agreement is fairly good in all cases. The estimation for PVOH was within the range of experimental values. The δ of PVAC was underestimated by 7% with respect to the lower value of the experimental range, while for PA6 it was overestimated by 9%.

An amorphous cell of a h88-PVAC/PA6 mixture at 1/1 composition is shown in Figure 2 as a typical example of the systems studied. The system contains 1324 atoms. The PA6 and the h88-PVAC chains are colored black and white, respectively. Grey shading is used to show the VAC groups on the polyvinyl chains. The hydrogens have been omitted for clarity. The tendency of the polymers to *mix* at a specific composition was estimated via the cohesive energies of the mixtures and the pure components. These are shown in Figure 3 as a function of the PA6 volume fraction. In all cases the values referring to blends were between the pure component values. For the h75-PVAC/PA6 blend, the above was valid within the error bars. Subsequently, the χ parameters were estimated as

$$\chi = \left(\frac{\Delta E_{\mathrm{mix}}}{RT}\right) V_{\mathrm{mon}} \tag{9}$$

where V_{mon} is a monomer unit volume. Here, it was taken arbitrarily equal to the smaller monomer volume for each blend. For the blends of PVAC/PA6 it was V_{mon} = 72.3 cm^3/mol and for the other mixtures V_{mon} = 35 cm^3/mol.[19] ΔE_{mix} for a binary mixture is defined as[33]

$$\Delta E_{\mathrm{mix}} = \phi_1 \left(\frac{E_{\mathrm{coh}}}{V}\right)_{\mathrm{pure1}} + \phi_2 \left(\frac{E_{\mathrm{coh}}}{V}\right)_{\mathrm{pure2}} - \left(\frac{E_{\mathrm{coh}}}{V}\right)_{\mathrm{mix}} \tag{10}$$

where ϕ is the volume fraction and the indices pure and mix denote that the cohesive energy densities in parentheses refer to the pure components and to the binary mixture, respectively. χ as a function of the PA6 volume fraction is shown in Figure 4. The relatively large error bars are probably due to the higher number of trajectories required for estimating averages at such a low temperature. The convex curves drawn through the χ values show maxima around the 1/1 composition. This, presumably, results from the higher number of unfavorable (unlike) contacts between the two components since at this composition masses of equal volume of the two components are brought into contact. The χ values for the hydrolyzed PVAC mixtures were found between those of the PVOH and PVAC mixtures for a given composition. The higher χ parameters (lower compatibility) were observed for the PVOH mixtures. The insertion of VAC monomer units along the PVOH chains had a notable effect in decreasing the cohesive energy densities of the pure phases and mixtures with respect to the pure phase of PVOH and its mixtures (Figure 3) and consequently the Flory−Huggins parameters (Fig-

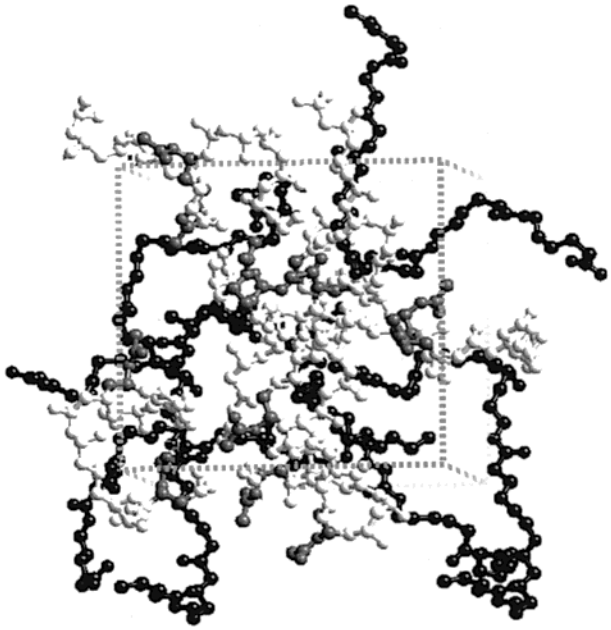

Figure 2. Amorphous cell of a h88-PVAC/PA6 mixture at 1/1 composition. The PA6 and the h88-PVAC chains are colored black and white, respectively. The light gray beads are the VAC groups of the h88-PVAC chains. Hydrogens are not shown for clarity.

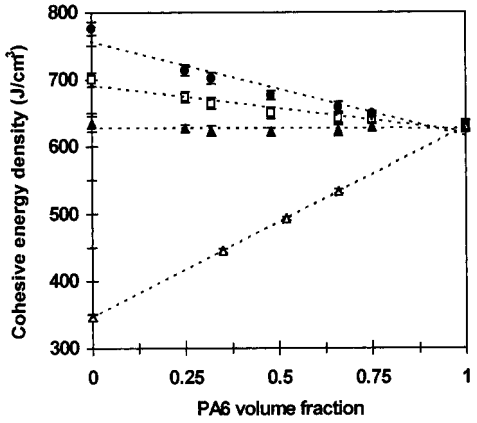

Figure 3. Cohesive energy density as a function of the PA6 volume fraction for the pure phases and mixtures of PVOH (circles), h88-PVAC (squares), h75-PVAC (filled triangles), and PVAC (open triangles).

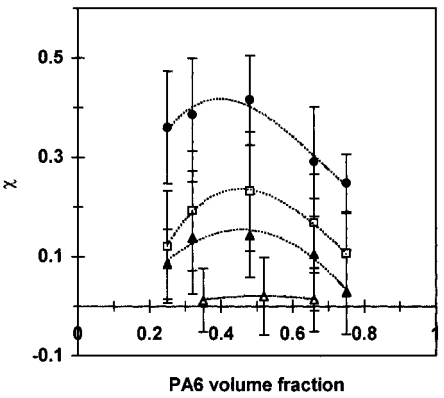

Figure 4. Flory−Huggins interaction parameter χ as a function of the PA6 volume fraction for the binary blends of PVOH (circles), h88-PVAC (squares), h75-PVAC (filled triangles), and PVAC (open triangles). The large error bars are attributed to the large number of trajectories required for the estimation of mean values at low temperature.

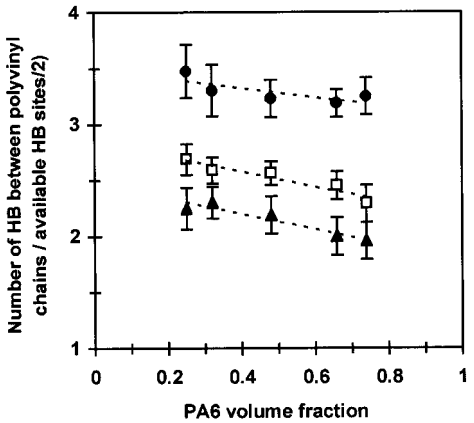

Figure 5. Fraction of total hydrogen bonds between the polyvinyl chains over the available sites on these chains for hydrogen bonding divided by 2, as a function of the PA6 volume fraction in the PVOH (circles), h88-PVAC (squares), and h75-PVAC (triangles) mixtures.

ure 4). It is, thus, deduced that as the number of VAC units in the backbone of PVOH chains increases the compatibility with the PA6 chains improves.

As depicted in Figure 4, the average values of χ are above zero in all cases with the lower values corresponding to the PVAC mixtures, for which they are very close to zero. These results conform with the observations reported in the literature that these mixtures do not develop particularly attractive interactions. According to refs 18 and 19, the χ for the h88-PVAC/PA6 mixture at $T = 221$ °C was estimated as −0.05 and in the range −0.027 to −0.055, respectively. These calculations were based on the simplified Nishi−Wang equation,[34] which correlates the χ with melting temperature data for the pure component and the blend, and the heat of fusion of the crystallizable component. In the present study, preliminary calculations at high temperature ($T = 221$ °C) gave for the mixture h88-PVAC/PA6 with composition 1/1 a value of χ equal to −0.06, in very good agreement with the above findings. For the mixture PVAC/PA6 with composition 1/1, the χ at the above temperature was estimated as −0.015. A detailed study of these blends at high temperature was beyond the scope of this work. However, it is evident that χ decreases as temperature rises, revealing increased compatibility. The small negative values of χ indicate limited compatibility for these mixtures.

To gain insight into how the chemical constitution of the polyvinyl chains affected the χ parameters, the ability of the different polyvinyl chains to form hydrogen bonds was examined. The intra- and intermolecular hydrogen bonds between the polyvinyl chains were measured by using the Viewer module of InsightII. The hydrogen bonds were bound to satisfy two criteria, namely that the distance between the proton on the donor atom and the acceptor atom should be less than a specified distance and that the angle formed between the donor, the proton, and the acceptor atom should be greater than 120°. Figure 5 depicts the fraction of total hydrogen bonds formed between the polyvinyl chains over the available sites for hydrogen bonding divided by two (since one bond involves two sites) as a function of the PA6 volume fraction in the PVOH, h88-PVAC, and h75-PVAC mixtures. For the results shown in Figure 5, the PA6 chains were subtracted from each system and only the hydrogen bonds formed by the polyvinyl chains were measured. For each VOH or VAC monomer unit, one site for hydrogen bonding was assumed (for the VAC monomer unit the oxygen attached to the backbone is much less available to form a hydrogen bond). It is mentioned that, for different types of mixtures, the number of available sites for hydrogen bonding was the same at the same composition. Figure 5 merely depicts the fact that, for each composition, as the number of VAC monomer units increases (going downward from PVOH to h88-PVAC and h75-PVAC) the ability of the chains to form hydrogen bonds decreases. This could result in less attractive intramolecular interactions between the vinyl chains and, thus, favor compatibility with the PA6 chains in the order PVOH < h88-PVAC < h75-PVAC. In the course of one series, the data seem to fall on a line with a small negative slope. This could simply be attributed to a decreased number of polyvinyl chains in the direction of higher PA6 composition.

It is noted, here, that calculation of the average hydrogen bonds between the different components in the above mixtures yielded unreliable results with big noise. No specific trend was found for the intermolecular hydrogen bonds with respect to the composition or the hydrolysis degree of the PVAC chains. This is probably due to the low temperature of examination, where the number of contacts between the different components depends on the initial distribution of the chains in the amorphous phase (initial mixing).

Furthermore, the dihedral distribution of the polyvinyl chains was calculated for the PVOH, h88-PVAC, and h75-PVAC mixtures for the compositions 2/1 and 1/2. Only the dihedral angles formed by the backbone carbon atoms were considered in this calculation. The estimation of the average population in the trans, gauche+, and gauche− states was performed by integration of the area under the dihedral distribution curves (not shown here) for each trajectory and averaging over all trajectories created for a specific composition. The conformations of the VAC-containing chains were expected to be more extended compared to the PVOH chains because of the bulky pendant groups of the VAC monomer units. Indeed, it was found that for the mixture 2/1 the average population in the trans state was around 55 ± 7%, 61 ± 5%, and 67 ± 4%, for the PVOH, h88-PVAC, and h75-PVAC mixtures, respectively. Similarly, the corresponding values for the 1/2 composition were 55 ± 5%, 64 ± 6%, and 70 ± 6%. These observations corroborate the

assumption of a more open intramolecular structure of the acetylated chains.

3.2. Mesoscopic Simulations. At the mesoscopic level, the model Gaussian chains stood for high MW polymers. The representation was coarse-grained and the atomistic details were accounted for, implicitly, in the size and interaction parameters of the Gaussian chains (section 2.3.2). After setting up the initial configurations, the systems were let to evolve toward equilibrium (phase separation or mixing). More specifically, the initially homogeneous phases (one phase region in the phase diagram) were cooled (in the two phase region) by turning on the interactions at time $t = 0$. The kinetics of phase separation were examined first and then the mixture compatibility was deduced from the final equilibrium morphologies.

A. Kinetics. A common practice in the study of the kinetics of phase separation is the calculation of the structure factor $S(\mathbf{q},t)$ ($\mathbf{q}$ is the scattering vector equal to $(4\pi/\lambda)\sin(\theta/2)$, where λ and θ are the wavelength of light and the scattering angle, respectively), at regular time intervals. This was calculated as the angle-averaged square modulus of the Fourier transform of a density field $\rho_I(\mathbf{r},t)$. An example is given in Figure 6 where the amplitude is plotted vs $\mathbf{q}$ for the PVOH component of the PVOH/PA6 mixture (top) and the h75-PVAC/PA6 mixture (bottom), both at composition 2/1 after 500, 4000, and 8000 time steps. The amplitude increases and sharpens with time and the maximum peak moves toward smaller $\mathbf{q}$ as the size of the domains increases. The two systems in Figure 6 differ only in the χ interaction parameter and consequently in the temperature of the quench; i.e., the h75-PVAC mixture is cooled to a higher temperature compared to the PVOH/PA6 mixture since the χ of the former is lower (see Table 1 and Figure 4) and $\chi \sim T^{-1}$. If the amplitudes and the corresponding wavelengths of Figure 6 are compared for the two systems at the same time step, it can be seen that the amplitude of the h75-PVAC mixture is higher and it is displaced toward smaller $\mathbf{q}$, indicating a larger domain size due to thermal fluctuations.

The kinetics of domain growth are usually described by the time evolution of the domain size $R(t)$ which is defined as the inverse of the mean of $\mathbf{q}$ weighted by the $S(\mathbf{q},t)$

$$R(t) = \frac{\int \mathrm{d}\mathbf{q}\ S(\mathbf{q},t)}{\int \mathrm{d}\mathbf{q}\mathbf{q}\ S(\mathbf{q},t)} \qquad (11)$$

It has been shown that $R(t)$ grows as t^{α} where the exponent α takes distinct values depending on the stage of the phase separation (early, intermediate, or late stage), and the composition of the mixture (symmetric and asymmetric quenches). For a binary fluid the exponent at early times is $^1/_3$ and crosses over to $^2/_3$ or 1 at later times when hydrodynamic effects become important (Lifshitz−Slyozov[35]). In Figure 7 is plotted the log $R(t)$ vs log t for the polyvinyl phase of the PVOH, h88-PVAC, and h75-PVAC mixtures at compositions 1/1 (top) and 2/1 (bottom). Because of the absence of hydrodynamic modes in the current mesoscopic model, the crossover is not observed, instead all the simulation points fall in a straight line. A line with slope equal to $^1/_3$ has been drawn for comparison. This value is generally reported for spinodal decomposition via a diffusion mechanism.[36] For the systems under consideration the actual slopes ranged from 0.2 to 0.22 for the composition 1/1 and from 0.2 to 0.28 for the composition 2/1. The slightly higher slope in the case of the 2/1 mixture might be due to the fact that the polyvinyl chains are now the majority phase. In all cases the domain size $R(t)$ seems to decrease by increasing the hydrolysis degree of the polyvinyl chains. As discussed previously, a high hydrolysis degree correspondsto a more deep quench since the χ parameter is larger. Thus, for a specific time step the domain size is smaller for the more hydrolyzed mixtures, or in other words for quenches at lower temperatures.

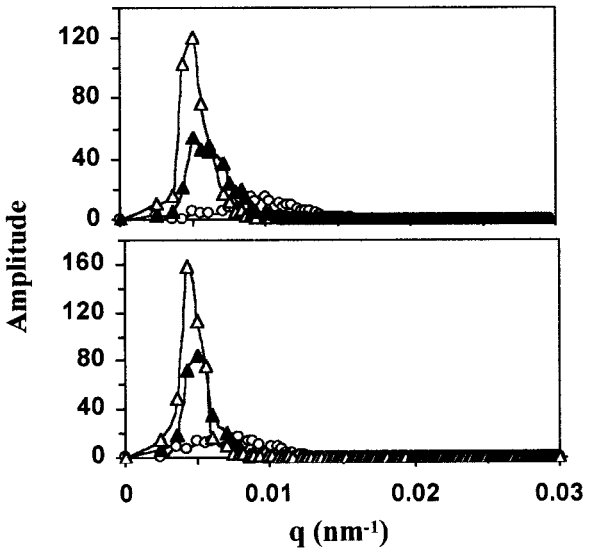

Figure 6. Structure factor of the polyvinyl chains vs the wavelength for the PVOH/PA6 mixture (top) and the h75-PVAC/PA6 mixture (bottom) both at composition 2/1, after 500 (open circles), 4000 (filled triangles), and 8000 (open triangles) time steps.

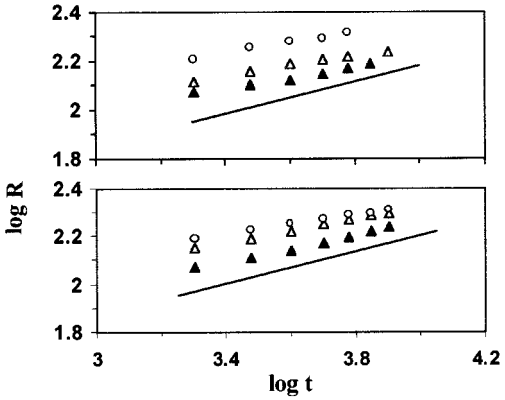

Figure 7. The log of the domain size $R(t)$ vs log t for the compositions 1/1 (top) and 2/1 (bottom) of the h75-PVAC/PA6 (open circles), h88-PVAC/PA6 (open triangles), and PVOH/PA6 (filled triangles) mixtures. A line with slope $^1/_3$ has been drawn for comparison.

B. Compatibility. For each type of bead and for each system, an average order parameter P was calculated as the deviation from the mean bead density at homogeneity[13]

$$P_{\mathrm{I}} = \frac{1}{V}\int_V [\theta_I^2(\mathbf{r}) - \theta_{I,0}^2]\ \mathrm{d}\mathbf{r} \qquad (12)$$

where θ is a dimensionless density (volume fraction), and the index 0 denotes average values at homogeneity.

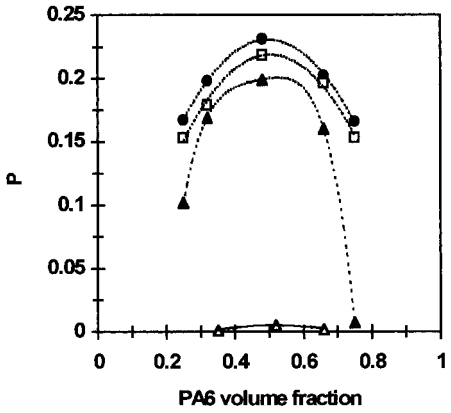

Figure 8. Mesophase order parameter P as a function of the PA6 volume fraction in the PVOH (circles), h88-PVAC (squares), h75-PVAC (filled triangles), and PVAC (open triangles) mixtures.

The order parameter P of the polyvinyl chains as a function of PA6 volume fraction for all binary blends considered here, is shown in Figure 8. P decreases in the same order as χ, i.e., toward a low PVAC hydrolysis degree for a given composition, and for compositions rich in either component. A decrease in P indicates better compatibility, or miscibility at shorter length scales, as the polymer phases mix more randomly. Blends with P values exceeding 0.1 gave macrophase separation. As an example of a macroscopically separated mixture in Figure 9, parts a and b are shown the density profiles of the h88-PVAC/PA6 mixture at composition 1/2 after 1000 and 5000 time steps (2400 and 12000 μs), respectively. Slices of the density profile at three faces of the periodic box are shown. The periodic boundary conditions are evident in these figures. In the case of phase separation the density spectrum is very broad. In all blends with P higher than 0.1, the density range that each component spanned was between 0 and 1. In Figure 9, parts a and b, the gray color corresponds to areas which contain only PA6 ($\rho_{PA6} = 1$) while the black areas correspond to the other component ($\rho_{PA6} = 0$). The zones of lighter shading constitute the interfaces which are occupied by both components. The size of these interfaces was measured between 10 and 30 nm, which corresponds to one or two cells. The phase separation proceeds via the diffusion of components through the interfaces. In Figure 9a, the phase separation has already started and interconnected zones appear while others remain dispersed in the PA6 phase. In Figure 9b, the phase separation is complete.

Parts a and b of Figure 10 show the evolution of the density profile of the h75-PVAC/PA6 mixture at composition 3/1 after 2000 and 16000 time steps (4800 and 38400 μs), respectively. The color notation is the same as in Figure 9. The order parameter of the h75-PVAC phase is around 0.1 (Figure 8). The density spectrum is as broad as before but in this case the phases formed by the PA6 chains (gray color) remain dispersed in the h75-PVAC phase, even after a long simulation time (Figure 10b). This is probably due to the low concentration of the PA6 chains in the mixture along with a small interaction parameter. The morphology in Figure 10, parts a and b, is reminiscent of the nucleation and growth mechanism during polymer phase separation.[37] The inclusion of hydrodynamics would facilitate the process of diffusion and coalescence of the phases and, thus, would help the system to find the right final

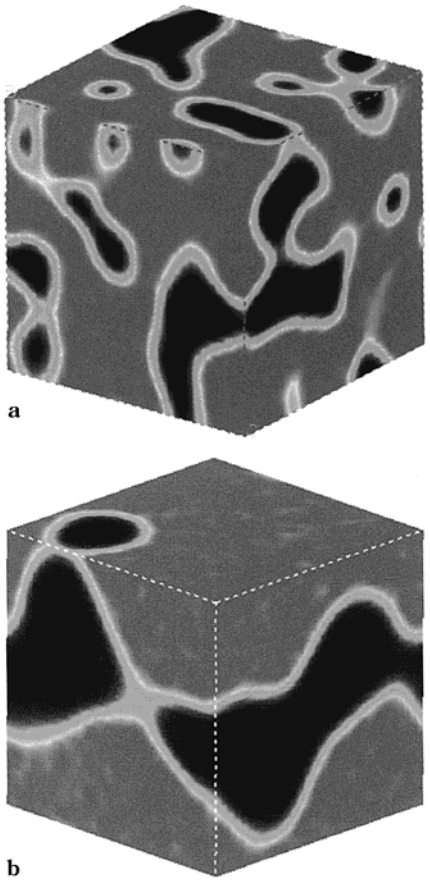

Figure 9. PA6 density profile slices, on three sides of the periodic box, for the h88-PVAC/PA6 mixture at composition 1/2. The gray color areas contain pure PA6 ($\rho_{PA6} = 1$), the black color areas contain the other component, and the light shading corresponds to the interface between them. Key: (a) snapshot after 1000 and (b) 5000 time steps, where the phase separation is complete.

morphology. Hydrodynamics has proven to be important, especially in the late stages of phase separation where the phases formed act as a barrier to further diffusion.[38]

For all PVAC/PA6 blends and the h75-PVAC/PA6 mixture at composition 1/3, the order parameter of the polyvinyl phase was close to zero. For these systems, the density of the components varied around the average value at homogeneity. The range of this variation becomes narrower as the interaction parameter becomes smaller. This can be understood in terms of the higher affinity between the components which, in turn, facilitates mixing in shorter length scales. Here, all χ parameters were above zero, and the variation of the density of each component around the mean value was approximately 21%.

The results reported herein are in line with internal experimental findings and with results reported in the literature. Transmission electron microscopy (TEM) measurements were conducted in our lab[39] for the PVOH/PA6 and h88-PVAC/PA6 mixtures, at composition 1/3. The polymer blend samples were prepared by treatment with OsO_4 in an aqueous phase. The OsO_4 marked selectively the polyvinyl phase, which can be observed clearly in Figure 11, parts a and b, for the PVOH and h88-PVAC mixtures, respectively. A length scale is given at the bottom of these pictures. In the case of the h88-PVAC mixture, the black nodules, which

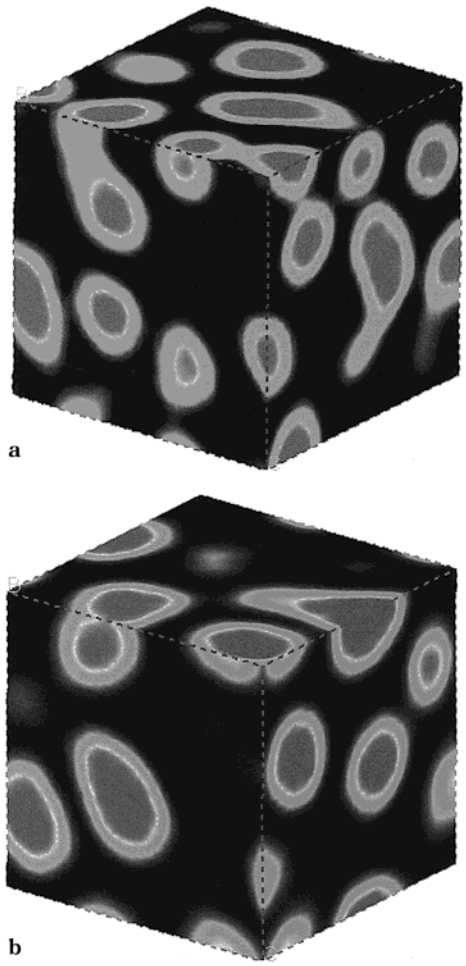

Figure 10. PA6 density profile slices for the h75-PVAC/PA6 mixture at composition 3/1, after (a) 2000 and (b) 16000 time steps. The notation of the colors is the same as in Figure 9.

correspond to the polyvinyl phase, show an uneven distribution in the PA6 matrix. There are areas where the polyvinyl phase is *dissolved* in the PA6 matrix and others where the size of the nodules vary from 1 μm to some submicrometer values. Compared with the PVOH mixture where the nodules are even larger (the scale of observation is double), it becomes evident that the compatibility with PA6 is improved in the case of the h88-PVAC mixture. The size of the simulation box (around 0.4 μm at each side) permits a direct comparison with the TEM pictures in the case of the h88-PVAC mixture, whereas for the PVOH mixture the simulation is outside the length scale of TEM. Qualitatively, it can be said that the better mixing of PA6 with h88-PVAC observed by TEM is predicted here by a decrease in the χ parameter and a consequent decrease in the order parameter of this mixture with respect to the PVOH mixture at the same composition.

The incompatibility predicted for the PVOH/PA6 mixture compares well, also, with the results reported in ref 19. In the latter work, this type of mixture was found to be incompatible by revealing poor mechanical properties. In the same work, the data of T_g vs composition for the h88-PVAC/PA6 mixture, were approximated by an S-shaped curve. The parameters of this curve, that were determined by fitting to an empirical equation[40] were previously reported for block copolymer systems with strong tendency to segregate. However, in the same

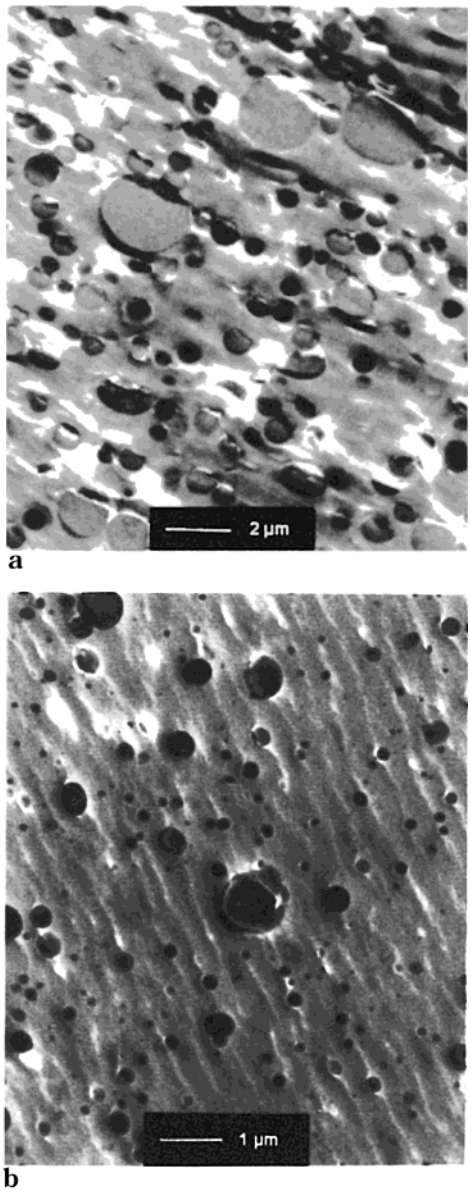

Figure 11. TEM pictures for (a) the PVOH/PA6 mixture and (b) the h88-PVAC/PA6 mixture, at composition 1/3. The observed nodules correspond to the polyvinyl phase.

work, this type of mixture, at compositions rich in PA6, was shown to have better mechanical properties with respect to the PVOH mixtures, indicating improved compatibility.

Furthermore, it was shown here, that higher acetylation of the PVOH chains (h75-PVAC) resulted in a decrease of the order parameter and miscibility was obtained for the mixture of composition 1/3, rich in PA6. It can be, thus, concluded that the acetylation of the PVOH chains facilitates mixing with PA6, especially for compositions rich in PA6.

4. Conclusions

A hierarchical approach was presented for the study of binary blend compatibility of PA6 with PVOH, PVAC, and partially hydrolyzed PVAC, for a wide range of compositions, at $T = 298$ K. The Flory−Huggins interaction parameter χ for oligomers of the above systems was derived as a function of composition, from MD atomistic simulations. For all mixtures, the highest χ were

observed for the 1/1 composition. The PVAC/PA6 mixtures had the smallest, close to zero, χ for all compositions examined, while the highest values were obtained for the PVOH/PA6 mixtures. The χ parameters for the hydrolyzed PVAC/PA6 mixtures were found between the two. Hence, on a χ basis, improved mixture compatibility was predicted in the direction of increased content of acetate groups (low hydrolysis degree) at a specific composition and for compositions rich in either component. The influence of the hydrolysis degree on the mixture compatibility was explained in terms of the reduced ability of the acetylated chains to form intramolecular hydrogen bonds and in terms of the bulky side groups that resulted in more extended conformations (more open structure) of these chains. Preliminary calculations at high temperature ($T = 221$ °C) gave for the mixture h88-PVAC/PA6 with composition 1/1, a χ value equal to -0.06 in agreement with values reported by others.[18,19] The small values of χ indicated that even at high temperature the compatibility of these mixtures is limited.

The cohesive interactions and other atomistically derived parameters were supplied to coarse-grained simulations. At these mesoscopic simulations, the dynamic evolution of phase separation of high MW blends was observed over time scales on the order of some microseconds. The structure factor and the rate of domain growth were examined as a function of hydrolysis degree. It was found that for mixtures of the same composition the domain size at a specific time step was smaller for mixtures having a higher hydrolysis degree and consequently higher χ interaction parameter (quench at lower temperature). The exponent of the domain growth was found to vary between 0.2 and 0.28 compared to the value $^1/_3$ that is predicted for spinodal decomposition via diffusion. In terms of compatibility, only mixtures having very small, close to zero, χ parameters were found compatible. This is explained by the negligible entropy that high polymers gain upon mixing and the consequent need for very favorable interactions in order to mix. The incompatible mixtures gave macrophase separation with density profiles of each component varying between 0 and 1. The order parameter of the phases formed were shown to decrease in the order PVOH < h88-PVAC < h75-PVAC < PVAC, for a given composition, indicating that the acetylation of the PVOH chains facilitates mixing with PA6. This trend was found to compare well with internal TEM measurements, and with results reported in the literature. The mixture of h75-PVAC for the composition $^1/_3$-rich in PA6, and all the PVAC mixtures were found compatible with order parameters close to zero. For these mixtures, the density spectrum of each component was around the average value at homogeneity.

Acknowledgment. The authors wish to thank Rhodia Recherches for permitting the publicationof this work. Philippe Menez is gratefully acknowledged for supplying the TEM results. Dr. Dave Nicolaides, from MSI, is kindly acknowledged for helpful discussions. T. S. gratefully acknowledges the financial support of a TMR Marie-Curie grant (Contract No.: FMBICT983007).

References and Notes

(1) Helfand, E.; Wasserman, Z. R. *Macromolecules* **1976**, *9*, 879−888.
(2) Leibler, L. *Macromolecules* **1980**, *13*, 1602−1617.
(3) Melenkevitz, J.; Muthukumar, M. *Macromolecules* **1991**, *24*, 4199−4205.
(4) Matsen, M. W.; Schick, M. *Phys. Rev. Lett.* **1994**, *72*, 2660−2663; *Macromolecules* **1994**, *27*, 6761−6767.
(5) Matsen, M. W.; Bates, F. S. *Macromolecules* **1996**, *29*, 1091−1098.
(6) Matsen, M. W.; Schick, M. *Curr. Opin. Colloid Interface Sci.* **1996**, *1*, 329−336.
(7) Bates, F. S.; Fredrickson, G. H. *Phys. Today* **1999**, *52* (2), 32−38.
(8) Fraaije, J. G. E. M. *J. Chem. Phys.* **1993**, *99*, 9202.
(9) Fraaije, J. G. E. M.; van Vlimmeren, B. A. C.; Maurits, N. M.; Postma, M.; Evers, O. A.; Hoffmann, C.; Altevogt, P.; Goldbeck-Wood, G. *J. Chem. Phys.* **1997**, *106*, 4260−4269.
(10) Hoogerbrugge, P. J.; Koelman, J. M. V. A. *Europhys. Lett.* **1992**, *19*, 155−160; *Europhys. Lett.* **1993**, *21*, 363−368.
(11) Groot, R. D.; Warren, P. B. *J. Chem. Phys.* **1997**, *107*, 4423−4435.
(12) Groot, R. D.; Madden, T. J. *J. Chem. Phys.* **1998**, *108*, 8713−8724.
(13) van Vlimmeren, B. A. C.; Maurits, N. M.; Zvelindovsky, A. V.; Sevink, G. J. A.; Fraaije, J. G. E. M. *Macromolecules* **1999**, *32*, 646−656.
(14) Zheng, S.; Huang, J.; Liu, W.; Yang, X.; Guo, Q. *Eur. Polym. J.* **1996**, *32*, 757−760.
(15) Nir, Y.; Narkis, M.; Siegmann, A. *J. Macromol. Sci.—Phys.* **1998**, *B37*, 863−882.
(16) Uno, M.; Norton, L. J.; Kramer, E. J.; Oda, H. *J. Mater. Sci.* **1998**, *33*, 853−858.
(17) Ahn, T. O.; Kim, C. K.; Kim, B. K.; Jeong, H. M.; Huh, J. D. *Polym. Eng. Sci.* **1990**, *30*, 341−349.
(18) Ha, C−S.; Lee, W−K.; Roe, T−W.; Cho, W−J. *Polym. Bull.* **1993**, *31*, 359−365.
(19) Koulouri, E. G.; Kallitsis, J. K. *Polymer* **1998**, *39*, 2373−2379.
(20) Theodorou, D. N.; Suter, U. W. *Macromolecules* **1985**, *18*, 1467.
(21) Meirovitch, H. *J. Chem. Phys.* **1983**, *79*, 502.
(22) Rigby, D.; Sun, H.; Eichinger, B. E. *Polym. Int.* **1997**, *44*, 311−330.
(23) Greengard, L.; Rokhlin, V. I. *J. Comput. Phys.* **1987**, *73*, 325.
(24) Schmidt, K. E.; Lee, M. A. *J. Stat. Phys.* **1991**, *63*, 1223−1235.
(25) Ding, H. Q.; Karasawa, N.; Goddard, W. A., III. *J. Chem. Phys.* **1992**, *97*(6), 4309−4315.
(26) van Krevelen, D. W. *Properties of Polymers*; Elsevier: New York, 1976.
(27) de Gennes, P. G. *Scaling Concepts in Polymer Physics*; Cornell University: Ithaca, NY, 1979.
(28) Doi, M.; Edwards, S. F. *The Theory of Polymer Dynamics*, Clarendon: Oxford, England, 1986.
(29) Maurits, N. M.; Zvelindovsky, A. V.; Fraaije, J. G. E. M. *J. Chem. Phys.* **1998**, *108*, 9150−9154.
(30) Kawasaki, K.; Koga, T.; Kawakatsu, T. *Mater. Res. Soc. Symp. Proc.* **1992**, *237*, 87.
(31) Press, W. H.; Flannery, B. P.; Teukolky, S.; Vetterling, W. T. *Numerical Recipes*; Cambridge University Press: Cambridge, England, 1987.
(32) Bicerano, J. *Prediction of Polymer Properties*; Marcel Dekker, Inc.: New York, 1993.
(33) Case, F. H.; Honeycutt, J. D. *TRIP* **1994**, *2*, 259−266.
(34) Nishi, T.; Wang, T. T. *Macromolecules* **1975**, *8*, 909.
(35) Lifshitz, I. M.; Slyozov, V. V. *J. Phys. Chem. Solids* **1961**, *19*, 35.
(36) Coveney, P. V.; Novik, K. E. *Phys. Rev. E* **1996**, *54*, 5134.
(37) Bates, F. S. *Science* **1991**, *251*, 898−905.
(38) Groot, R. D.; Madden, T. J.; Tildesley, D. J. *J. Chem. Phys.* **1999**, *110*, 9739−9749.
(39) Menez, P. Rhodia Recherches, private communication.
(40) Lin, A. A.; Kwei, T. K.; Reiser, A. *Macromolecules* **1989**, *22*, 4112.

MA001669T